ACI STRUCTURAL JOURNAL TECHNICAL PAPER

Title no. 88-S40

Shear-Friction Tests on Reinforced Concrete Panels

by Frank J. Vecchio and Mauricio Nieto

An experimental investigation is described in which reinforced concrete panels were tested under conditions approximating shear-friction behavior. A principal shear plane region provided in each panel was uniaxially reinforced and transversely precracked. Uniform edge loads applied to the panels were of varying ratios of shear to normal stress. The load-resisting mechanism typically observed to develop across the shear plane was one involving strut action. The influence of the preexisting transverse cracks was minimal, while that of externally applied normal stresses was substantial. The modified compression field theory, incorporated into a nonlinear finite element analysis procedure, was found to predict accurately strength and load-deformation response under these aberrant conditions. Design code formulations, based on shear-friction concepts, gave from highly conservative to unconservative estimates of strength.

Keywords: concrete panels; deformation; finite element method; **friction; reinforced concrete; shear tests**; strength; structural design.

The modified compression field theory (MCFT) was proposed several years ago as a simple theoretical model for predicting the response of reinforced concrete elements subjected to in-plane shear and normal stresses.[1] The theory was based on the smeared-crack concept with equilibrium, compatibility, and stress-strain relations formulated in terms of average strains and average stresses. New constitutive relations were developed for cracked concrete, reflecting significant influences from compression strain softening and tension-stiffening effects. Consideration was also given to the transfer of stresses across cracks. Subsequently, the formulations of the MCFT were incorporated into a nonlinear finite element program.[2]

In reinforced concrete structures subjected to shear, various internal mechanisms can be created to resist load. In regions where the reinforcement and ensuing crack conditions are well distributed, the predominant mechanism of resistance is internal truss action. Through the formation of diagonal cracks, compression struts develop in the concrete while the longitudinal and transverse reinforcement act as tension ties. The MCFT, formulated to specifically model this behavior, has been shown to provide accurate predictions of response under such conditions.[1,2]

Situations arise, however, where it would be inappropriate to assume the formation of a well-distributed crack condition. This can occur, for example, at the interface of precast and cast-in-place concrete, in cross sections weakened by cracking, or in structural components under high direct shear, such as corbels and ledger beams. In such cases, strength can be governed by behavior along a single plane or dominant crack. Here, the mechanism of shear transfer is commonly seen as relying less on the formation of compression fields, and more on contributions from shear friction, dowel action, and aggregate interlock.

An experimental investigation was undertaken in which reinforced concrete panels, loaded in shear, would be governed by behavior along a precracked, uniaxially reinforced shear plane. The primary objective was to examine the ability of MCFT-based formulations to accurately predict response under these conditions. Also of interest were the shear strengths and shear transfer mechanisms developed, and a comparison of strengths to those predicted by shear-friction models.

RESEARCH SIGNIFICANCE

Modified compression field theory concepts in various forms have been adopted by numerous researchers and applied to a wide variety of problems. The experimental and analytical work reported herein will help to define the range of applicability and the limitations of the theory under conditions deviating from those implicitly assumed.

EXPERIMENTAL PROGRAM

The experimental program undertaken involved the testing of six reinforced concrete panels under various conditions of monotonic in-plane load. The panels were all of similar construction, and contained a uniaxially reinforced central test region. Prior to testing, transverse cracks were induced in the test panels by applying

ACI Structural Journal, V. 88, No. 3, May-June 1991.
Received Apr. 11, 1990, and reviewed under Institute publication policies.

*ACI member **Frank J. Vecchio** is an associate professor of civil engineering at the University of Toronto. A member of ACI Committees 435, Deflections of Structures, and 447, Finite Element Analysis, his research interests relate primarily to the constitutive modeling, nonlinear analysis, and computer-aided design of reinforced concrete.*

*ACI member **Mauricio Nieto** is a design engineer with Carruthers and Wallace Consulting Engineers of Toronto. He completed his undergraduate studies at the University of Costa Rica and earned his MASc at the University of Toronto.*

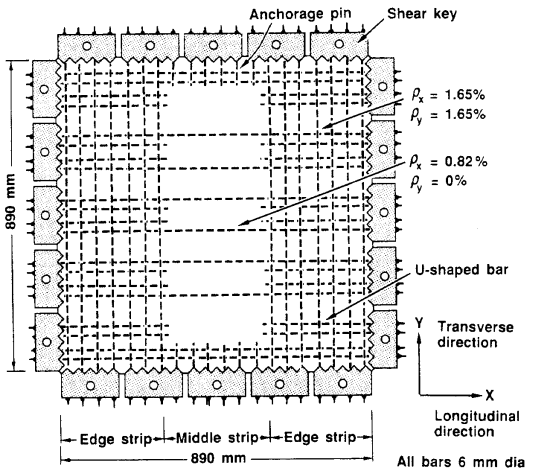

(a) Specimen Details

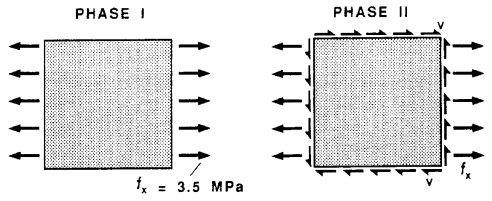

Panel No.	Phase I Loading	Phase II Loading (v : f_x : f_y)
PN1	No	1 : 0 : 0
PN2	Yes	1 : 0 : 0
PN3	Yes	1 : 0.5 : 0
PN4	Yes	1 : 1.0 : 0
PN5	Yes	1 : -0.5 : 0
PN6	Yes	1 : -1.0 : 0

(b) Loading Conditions

Fig. 1—Details of test panels

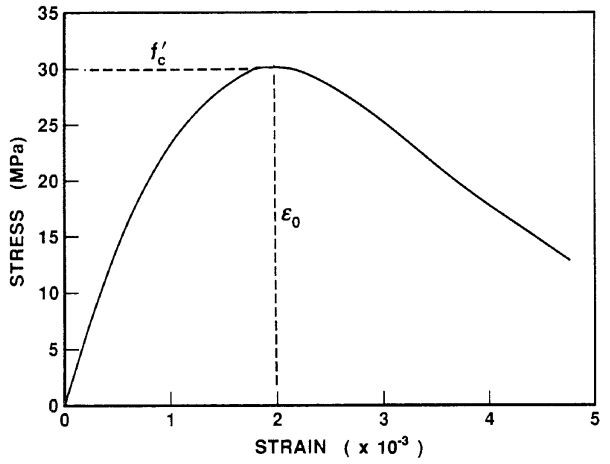

Panel No.	f'_c (MPa)	f_{sp} (MPa)	ε_0 ($x10^{-3}$)
PN1	33.5	3.2	2.1
PN2	29.8	2.8	1.9
PN3	29.9	3.0	1.9
PN4	32.8	3.0	2.1
PN5	32.6	2.9	2.0
PN6	27.6	2.6	2.0

(a) Concrete

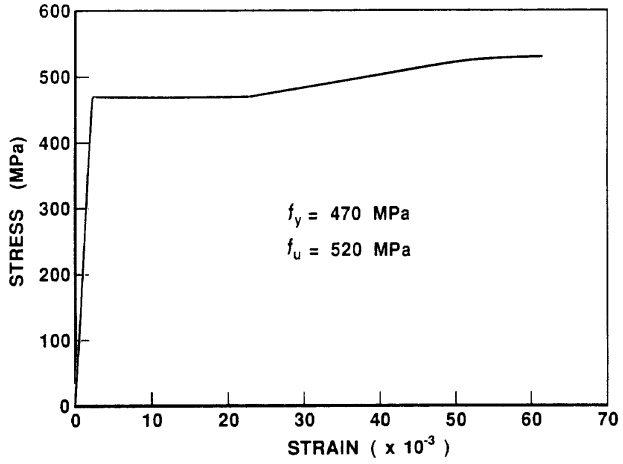

(b) Reinforcement

Fig. 2—Material stress-strain properties

uniaxial tensile loads. The panels were then subjected to various combinations of uniaxial tension or compression, and shear. The shear friction response of the panels, in the precracked and uniaxially reinforced region, was of primary interest.

The test specimens were 890 x 890 x 70 mm (35 x 35 x 2.75 in.) concrete panels reinforced with 6 mm (0.25 in.) nominal diameter deformed bar. The reinforcement detailing essentially divided the panel into three equal-area strips [see Fig. 1(a)]. The two edge strips were orthogonally reinforced with both the longitudinal and transverse reinforcement ratios ρ_x and ρ_y, equal to 0.0165. In the central region, the longitudinal reinforcement ratio was reduced to 0.00823, and no transverse reinforcement was provided. Short anchorage pins were used at the edges of the middle region, in the transverse direction, to insure adequate load transfer. The reinforcement was placed in four layers, with a clear cover of 6 mm (0.25 in.) provided to the outermost bar.

Normal density concrete was used to cast the panel specimens. The mix components were such as to provide a nominal compression strength of 30 MPa (4300 psi) at 7 days using rounded aggregate of 10 mm (⅜ in.) maximum size. Standard tests performed on 150 x 300 mm (6 x 12 in.) cylinders yielded the concrete material properties summarized in Fig. 2(a). The compressive stress-strain response shown was typical for the

concrete, and was determined using a strain rate of 0.022 x 10^{-3}/sec. Note that the tensile strengths shown were determined from split-cylinder tests.

The reinforcement bars used for each of the panels came from a single supply of 6 mm (0.25 in.) nominal diameter bar with a cross-sectional area of 25.6 mm^2 (0.040 $in.^2$). After heat-treating, the reinforcing steel exhibited a very ductile response with a yield stress of 470 MPa (68 ksi) and an ultimate stress of 520 MPa (75 ksi). A typical stress-strain curve, determined from tensile coupons at a strain rate of 0.02 x 10^{-3}/sec, is given in Fig. 2(b).

For load-application purposes, five shear keys per side were cast integrally with each panel. The reinforcing bars, machined to have threaded ends, passed through the shear keys and were fastened into place with nuts. The shear keys, in turn, fit into the shear rig test facility [see Fig. 3(a)]. This facility, described elsewhere,[1] allows panels to be loaded with any combination of proportional or nonproportional membrane shear and normal stress. The system of load application results in essentially uniformly applied stresses along the panel edges.

Surface strains were measured on both sides of a test panel using specially developed demountable mechanical strain gages with electronic feed-outs. Strain readings were taken in the longitudinal, transverse and two diagonal directions, at each load stage, from targets placed on a 300-mm (12-in.) grid over the middle strip of the panel [see Fig. 3(b)]. Linear variable differential transducers (LVDTs), mounted onto one side of the panel, also provided a continuous monitoring of average strain conditions [see Fig. 3(b)]. Electrical resistance strain gages, of 5 mm (0.2 in.) gage length, were applied onto the longitudinal reinforcement in the central test region [see Figure 3(c)]. These gave indications of local stresses in the reinforcing bars. The applied loads acting on the test panels were determined from pressure transducers on the hydraulic system, and from load cells installed onto the jacks.

Loads were applied to the test panels in a proportional and monotonic manner, up to failure. The loading regime imposed consisted of two phases. In the first phase of loading, a uniaxial tensile stress of 3.5 MPa (500 psi) was applied in the longitudinal direction. This served to precrack the specimens and thus establish shear friction planes. (Note: Panel PN1 was not subjected to this condition.) In the second phase of loading, combined shear and uniaxial normal stresses were applied in the proportions defined in Fig. 1(b). The load cases included pure shear, combined shear and compression, and combined shear and tension.

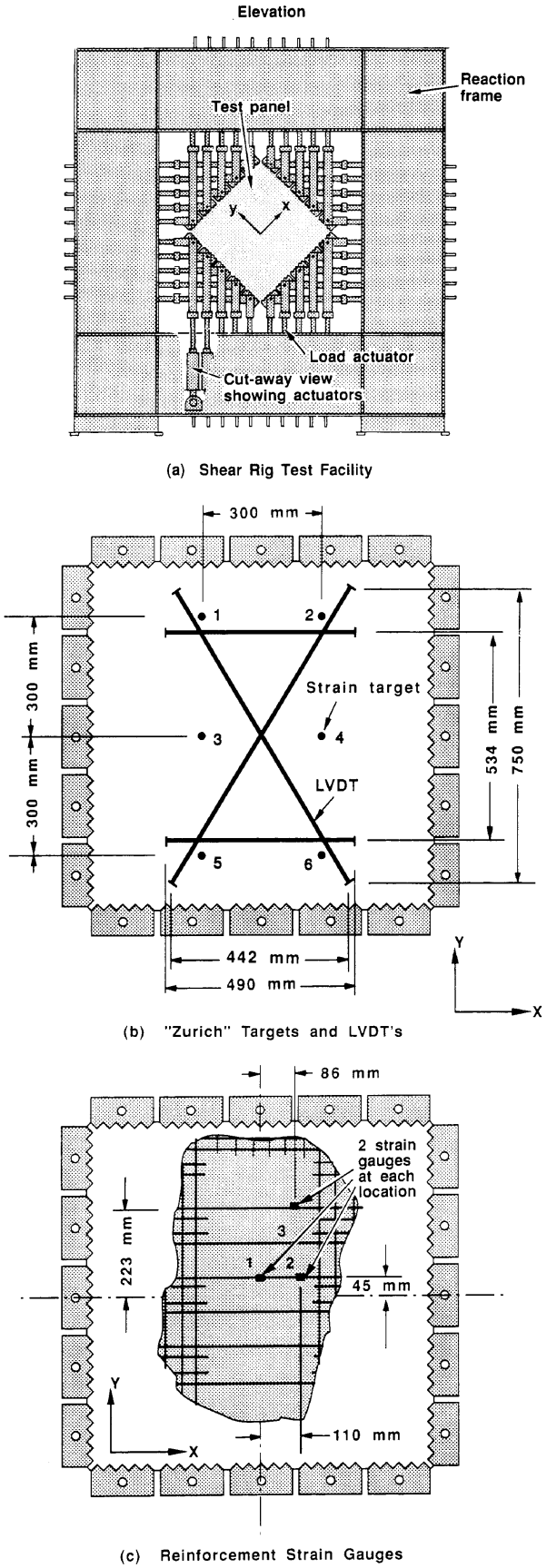

Fig. 3—Test setup and instrumentation

TEST OBSERVATIONS

For Panels PN2 through PN6, the first phase of loading resulted in a well-established pattern of cracks normal to the longitudinal reinforcement. These transverse cracks first appeared at a nominal tensile stress of 2.0 to 2.5 MPa (290 to 360 psi). At the maximum applied tensile stress of 3.5 MPa (500 psi), typically four or five full-length cracks had developed over the middle strip region of the panels [e.g., see Fig. 4(a)] with widths ranging up to 0.25 mm (0.010 in.). Mechanical

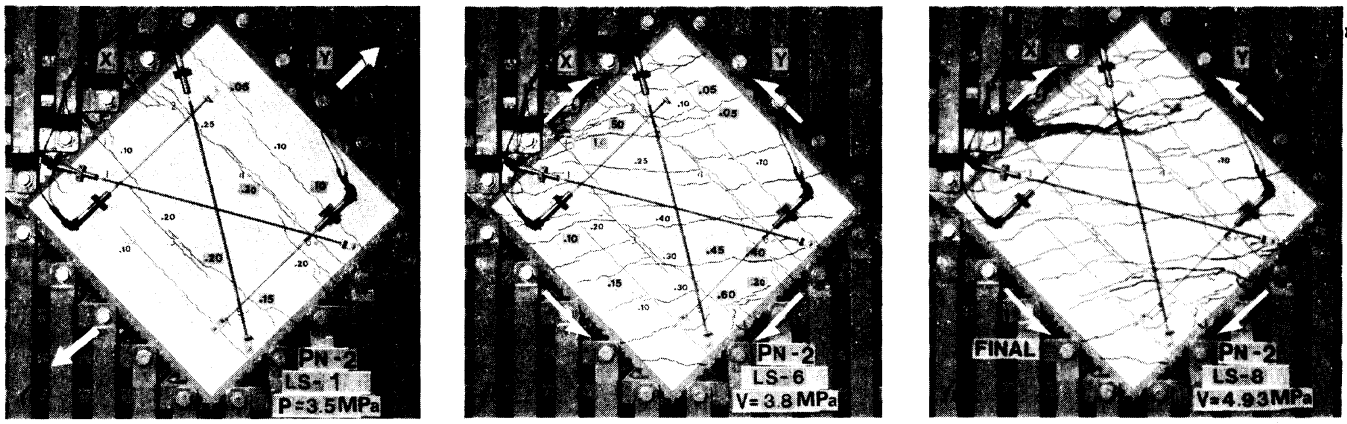

Fig. 4—Typical crack and failure conditions observed in test panels: (a) Panel PN2 loaded in uniaxial tension; (b) Panel PN2 under pure shear loading; and (c) Panel PN2 after failure

gage and reinforcing bar strain gage readings both indicated that the average tensile strain in the longitudinal direction was typically around 1.55×10^{-3}. Upon unloading, the cracks in the central region closed to a width of 0.05 mm (0.002 in). The corresponding residual longitudinal strain was 0.45×10^{-3}.

During the second phase of loading, the behavior of the previously formed transverse cracks depended largely on the load condition. In Panels PN5 and PN6, subjected to longitudinal compression and shear, the transverse cracks closed up shortly after loading commenced and remained closed throughout the test. In Panels PN3 and PN4, subjected to longitudinal tension and shear, segments of the transverse cracks opened up as loading progressed. Where the transverse cracks merged with newly formed diagonal cracks, crack widths of up to 1.5 mm (0.060 in.) were measured. In the case of pure shear, imposed on Panel PN2, no significant change in the residual width of the transverse cracks was observed.

The second phase of loading was characterized by the formation of diagonal cracks [see Fig. 4(b)]. In the panel edge strips, diagonal cracks formed at angles of between 25 to 45 deg with respect to the longitudinal direction, depending on the load condition. The cracks were relatively uniformly spaced at 100 mm (4.0 in.), with widths ranging between 0.05 and 0.15 mm (0.002 and 0.006 in.) at ultimate load. In the middle strip, the diagonal cracks formed predominantly at an angle of about 45 deg to the longitudinal axis, with an average spacing of between 120 and 200 mm (5.0 and 8.0 in.). Typically, a single dominant crack formed at the outer edges of the middle strip, with the width approaching 3.5 mm (0.140 in.) just before failure. Maximum crack widths in the center of the middle region ranged between 0.20 and 1.0 mm (0.008 and 0.040 in.), being larger in the cases of longitudinal tension and shear.

The failure mode of the panels was characterized by a tearing action along the principal crack near one edge of the middle strip. Two general types of failure were observed. In Panels PN2, PN3, and PN4, failure occurred after yielding had been achieved in all the longitudinal reinforcement crossing the middle strip. The failure condition occurred when the longitudinal bars crossing the dominant crack ruptured [see Fig. 4(c)]. In Panels PN5 and PN6, failure was governed by crushing of the concrete in the compressive strut adjoining the dominant crack. Some yielding of the longitudinal reinforcement occurred, but the bars did not rupture. In all panels, however, local crushing of concrete along crack interfaces was evident in the latter load stages. Panel PN1 did not achieve an ultimate load condition, failing prematurely due to pullout of a shear key.

The load-deformation responses of the panels are compared in Fig. 5(a) in terms of shear stress-shear strain behavior. The shear strains are derived from the mechanical strain gage readings averaged for the 300 mm (12 in.) wide middle strip; the shear stresses are equivalent to the nominal applied edge loads. Significant differences can be seen in the strength, stiffness, and ductility of the panels, as influenced by the longitudinal stresses. Panels PN2, PN3, and PN4, as a result of extensive yielding of the reinforcement, exhibited progressively more ductile response. Panels PN5 and PN6, conversely, demonstrated a stiffer load-deformation response and a more brittle failure as a result of the longitudinal compression. The ultimate shear strength of the panels also showed a large variation. The longitudinal tensile stresses imposed on Panels PN3 and PN4 resulted in decreases in shear strength of 22 and 42 percent, respectively, compared to the strength of Panel PN2. The longitudinal compression stresses present in Panels PN5 and PN6 resulted in a relative strength increase of about 13 percent.

The strains measured in the longitudinal reinforcement, in the center region, are shown in Fig. 5(b). The influence of the loading condition on the observed response is again seen to be significant. Also note that, for Panels PN5 and PN6, a reduction in longitudinal reinforcement strain was observed during the initial stages of loading. This was due to the closing of the initial transverse cracks. As diagonal cracks formed, the longitudinal strains began to increase once again. In the case of the panels under tension and shear, immediate increases in longitudinal strain resulted from a reopening of the transverse cracks.

Fig. 5(c) shows the inclination of the concrete principal tensile strain, in the middle strip region, calculated from the mechanical strain gage measurements. The principal strain direction ranged from 30 to 60 deg relative to the longitudinal axis, and again was dependent on the load condition. However, the diagonal cracks that formed in the middle regions remained reasonably close to 45 deg at all times. This anomaly suggests that some degree of slippage may have occurred along the crack interfaces.

DISCUSSION OF RESULTS

The test results indicate that panel behavior was not significantly influenced by the preexisting transverse cracks. Except for differences between the crack directions and the direction of the principal strains, little evidence was found to suggest that the slippage along transverse cracks was appreciable. Only in Panels PN3 and PN4 did the transverse cracks reopen, and then only in short segments near the top and bottom edges. Thus, effects of the initial transverse cracks on panel behavior were minor and limited primarily to the early stage of the load-deformation response. In all the specimens tested, however, extensive diagonal cracking developed. The indication was that the shear forces acting across the length of the middle strip were primarily resisted by truss action.

The influence of the longitudinal stresses on the panels' shear capacity was significant. Where failure was governed by yielding of the reinforcement, the externally applied longitudinal stresses had a direct influence on the shear strength. Axial tensile forces reduced the reinforcement's capacity for resisting shear, while compressive stresses increased capacity. However, the failure mode in the latter case was altered to one governed by crushing of concrete.

The heavily reinforced side regions of the panels also had a strong influence on behavior. They effectively restricted the middle region from expanding in the transverse direction, providing confinement and thus increasing shear capacity. Evidence of this effect can be found in comparing the tests results to those from corresponding panels tested by Bhide and Collins.[3] The Bhide and Collins panels were uniaxially reinforced throughout [see Fig. 6(a)]. Panel PB11, having a reinforcement ratio of $\rho_x = 0.01085$ and tested in pure shear, is suitable for comparison of Panel PN2. Similarly, Panel PB4 roughly corresponds to Panel PN4. Comparisons of the observed load-deformation responses are shown in Fig. 6(b) and 6(c). In the case of the PB-series of panels, failure occurred shortly after cracking. The PN-series panels, conversely, exhibited a ductile response after cracking with significantly higher ultimate strengths.

The panel strengths were also compared to the strengths predicted using the shear-friction provisions of ACI 318[4] and CSA A23.3 M84.[5] As seen in Fig. 7, the shear-friction model gave very conservative predictions for panels tested in pure shear, or in combined

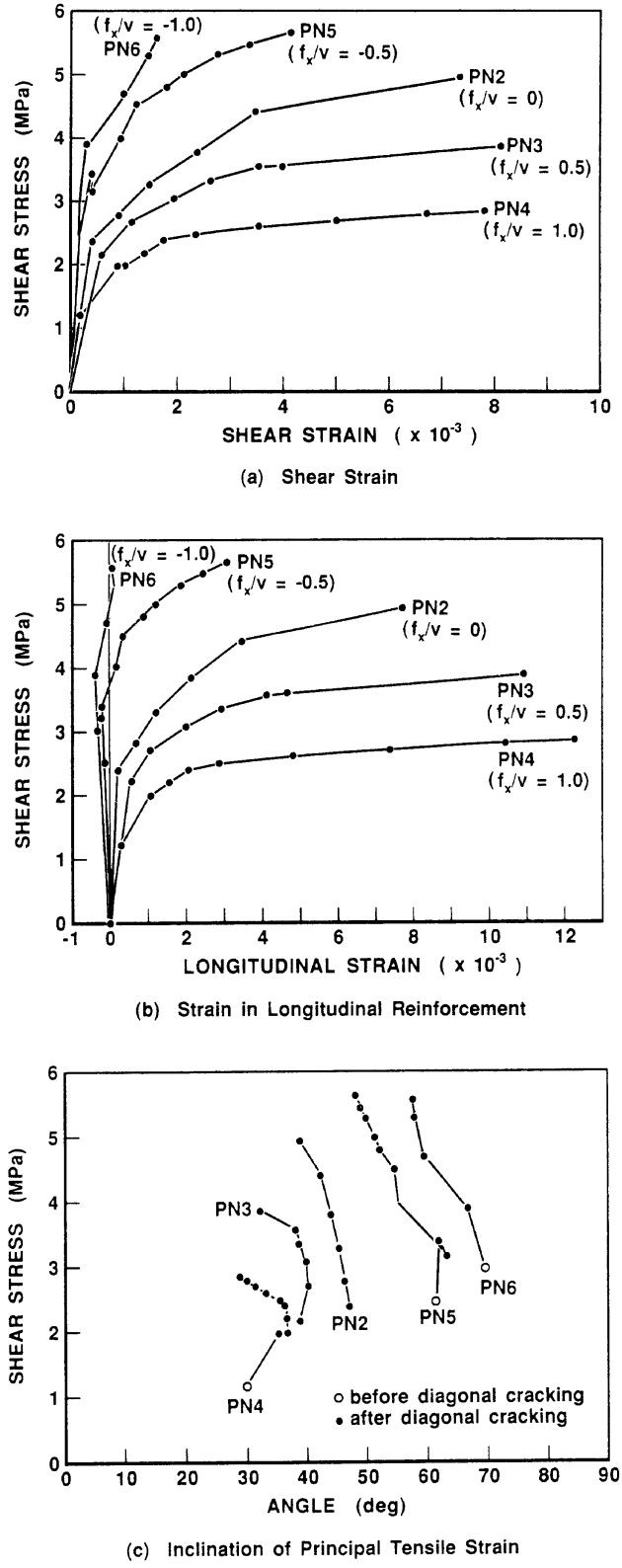

Fig. 5—Measured responses of test panels

shear and longitudinal tension. However, the predicted strengths became less conservative for panels loaded in shear and longitudinal compression. This is expected since the shear-friction model is based on the assumption that yielding of the reinforcement governs failure. Concrete crushing leading to failure, as occurred in the panels loaded in compression and shear, is not consid-

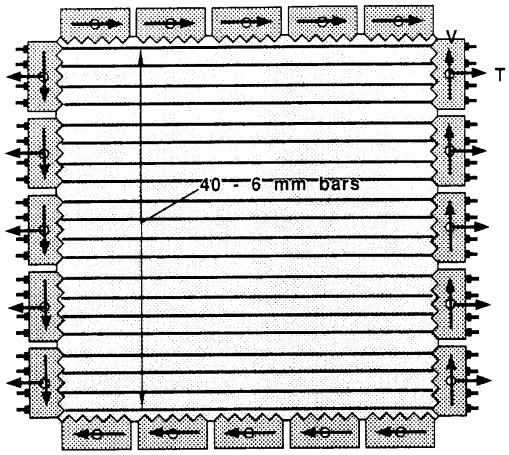

(a) Bhide and Collins Panels

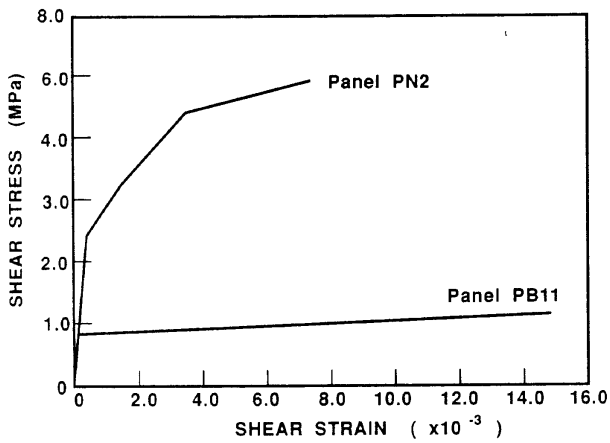

(b) Panels with Loading Ratio $f_x/v = 0$

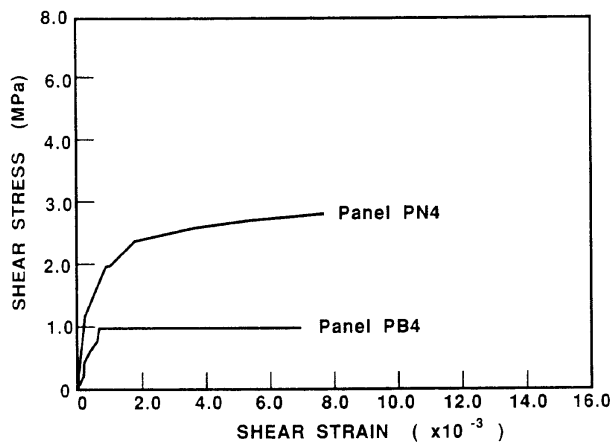

(c) Panels with Loading Ratio $f_x/v = 1$

Fig. 6—Comparisons to corresponding panels tested by Bhide and Collins[3]

ered except in defining arbitrary upper-bound limits for shear stress.

THEORETICAL RESPONSE

Theoretical predictions of the panels' response were obtained from nonlinear finite element analyses. The analysis program TRIX was used, which incorporates the concepts and constitutive relations of the modified

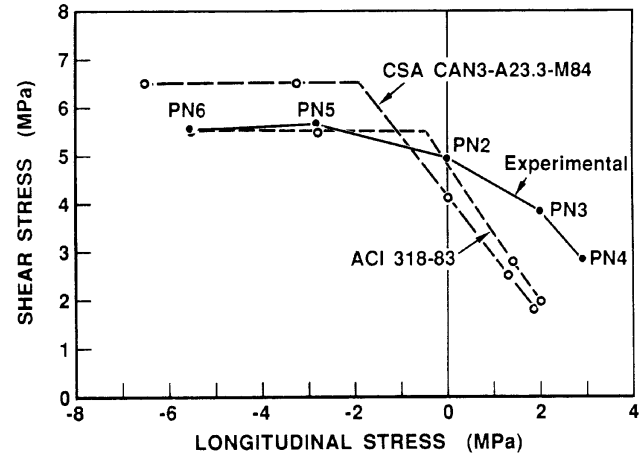

Fig. 7—Comparisons to strengths predicted by code specifications

compression field theory as described in Reference 2. The finite element algorithm is based on a smeared rotating crack modeling approach, employing a total-load secant-stiffness solution procedure.

The finite-element mesh used to represent the test panels, shown in Fig. 8(a), consisted of 120 rectangular elements. Element reinforcement was modeled in a smeared manner. In the two side-regions, the reinforcement ratios were set at $\rho_x = 0.0165$ and $\rho_y = 0.0165$. The reinforcement levels in the central region of the middle strip were $\rho_x = 0.00823$ and $\rho_y = 0$. In the edge regions of the middle strip, to reflect any influence from the anchorage pins, the reinforcement ratios were defined as $\rho_x = 0.00823$ and $\rho_y = 0.0203$. The concrete and reinforcement material strengths used were as determined from the test specimens. Distributed loads acting on the panel edges were represented as nodal forces. The effects of the initial transverse cracks, induced during the first phase of loading, were not represented.

The analyses indicated that the load-resisting mechanism developed within the panels involved compressive struts forming in the middle region between the two much stiffer side regions. The strut action was dominant through a band across the center of the panel, with the side regions of the middle strip being relatively ineffective. This is reflected, for example, in the nonuniform shear stress distribution determined for Panel PN2 at a shear stress of 3.0 MPa, shown in Fig. 8(b). The analyses further indicated that the stiff side regions provided a confinement effect, restricting the transverse expansion in the center region. This effect is evident in the computed transverse stresses shown in Fig. 8(c). The transverse compression induced in the middle strip led to the development of significantly higher strengths than would be obtained if the panel were uniaxially reinforced throughout. Thus, the much higher strengths obtained relative to the corresponding panels tested by Bhide and Collins is explained.

Fig. 9 compares the predicted and observed shear stress-versus-shear strain response of the panels, computed over a central region as previously described. In

general, very good agreement is seen in the post-cracking load-deformation response and in the ductility at ultimate load. The initial stiffnesses are overpredicted, partly due to the neglect of the preexisting transverse cracks. Fairly accurate predictions of the panels' ultimate strength and failure mode were also obtained. The ratio of the experimental to predicted ultimate shear strength, for the precracked panels, had a mean of 1.09 and a coefficient of variation of 9 percent. As can be seen in Fig. 9, the ultimate strengths were equally well-predicted over the complete range of longitudinal stresses considered. The predicted failure mode typically involved a shear failure of the concrete after yielding of the longitudinal reinforcement. In Panels PN5 and PN6, due to the longitudinal compression, yielding was localized and the failure was more brittle. These predictions agreed reasonably well with the observed failure modes. The behavior of Panel PN1 was not well-predicted because of test difficulties and the premature failure of the panel.

Also shown in Fig. 9 are panel responses predicted using a local nonlinear analysis approach. A linear elastic global analysis was first performed to obtain the stress distributions within the panel. Given the stresses on a particular element, a nonlinear local analysis was then performed to determine the element's strength and response. (Note: This is common procedure in the analysis of large structures.) It can be seen that this approach resulted in the prediction of element failure shortly after cracking, at loads much lower than were experimentally observed. The influence of nonlinear behavior on stress redistribution was not being taken into account.

Panel response was also examined in terms of longitudinal and transverse strains, inclination of the principal compressive strain direction, and stresses in the longitudinal reinforcement. Shown in Fig. 10, for example, are the predicted responses for Panel PN2. The longitudinal and transverse strains, and the inclination of the principal strain direction, were all reasonably well-predicted. For stresses in the longitudinal reinforcement, the experimental curve shows initial stresses present due to the preexisting cracks induced during the first phase of loading. These residual stresses were not modeled analytically. Otherwise, the reinforcement stresses were also predicted fairly accurately. Similar degrees of accuracy were obtained in the predicted response of the other panels.

To obtain another measure of the accuracy of the MCFT-based finite element procedure in predicting shear friction behavior, analyses were performed for initially uncracked pushoff specimens tested by Hofbeck, Ibrahim, and Mattock.[6] Program TRIX was once again utilized. The finite-element mesh shown in Fig. 11(a), comprised of 128 linear displacement elements, was used to model the specimens. The longitudinal reinforcing bars were modeled discretely using truss bar elements, whereas the transverse reinforcement (i.e., reinforcement crossing the shear plane) was modeled in a smeared manner. The analyses showed that, for the

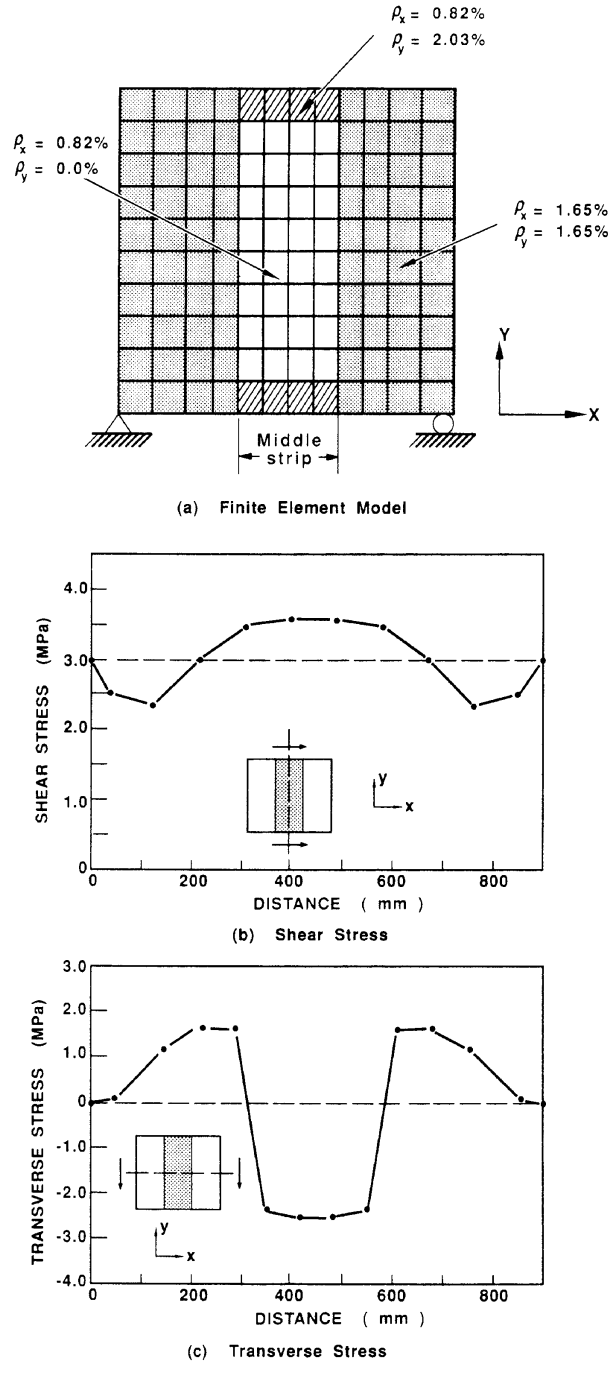

Fig. 8—Nonlinear finite element analysis of panels

lightly reinforced specimens ($\rho_x \leqslant 0.0088$), failure was governed by yielding of the reinforcement. For the more heavily reinforced specimens, the predicted failure mode involved a crushing of the concrete in the vicinity of the shear plane. Figure 11(b) compares the predicted ultimate strengths to the experimental values. Good accuracy is indicated, with a mean of 1.04 and a coefficient of variation of 10 percent, for the ratio of experimental to theoretical strength. The tendency to underestimate strength in the heavily reinforced specimens may be related to the influence of dowel action, which was not considered analytically.

Initially, in analyzing the pushoff specimens, the longitudinal reinforcement had been modeled in a

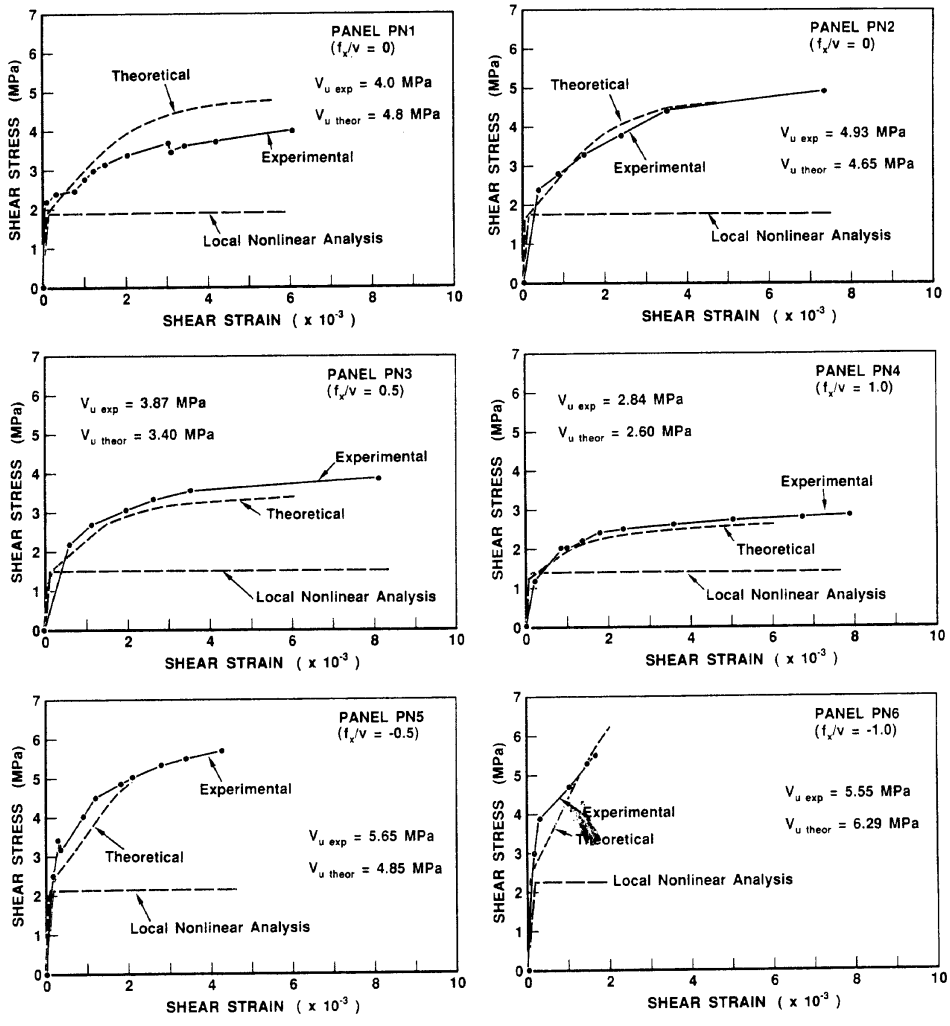

Fig. 9—Predicted load-deformation response of panels

smeared manner. The area of longitudinal reinforcement was equally distributed across the full width of the specimen, and thus the elements adjoining the shear plane were represented as being orthogonally reinforced. This led to significantly higher predictions of ultimate strength, and altered the crack formation and distribution of stresses. The indication is that, in structures where behavior is highly influenced by conditions at a well-defined shear plane, careful modeling of the reinforcement in adjoining regions is essential.

CONCLUSIONS

Reinforced concrete panels were tested to investigate the applicability of the modified compression field theory to situations deviating from the normally assumed conditions. The tests panels contained a shear plane region that was uniaxially reinforced and transversely precracked. The uniform load conditions applied included various combinations of shear and normal stress.

The preexisting transverse cracks showed little influence on the behavior of the panels. Little evidence of slippage was visible, although initial shear stiffnesses were somewhat reduced and local crushing of concrete along diagonal crack interfaces was observed. In all cases, a diagonal crack system formed and the longitudinal reinforcement yielded prior to ultimate load. Shear forces across the plane were resisted primarily through strut action, with failure being dictated by either rupturing of the reinforcement or crushing of the concrete struts. Externally applied stresses, acting normal to the shear plane, were found to significantly affect strength and load-deformation response.

The modified compression field theory, incorporated into a nonlinear finite element procedure, was used to model the test panels. It was found to predict accurately both the strength and load-deformation response of the panels. Initially uncracked pushoff specimens were also modeled, and their strengths were also well-predicted. However, in this case, the strength predictions were found to be sensitive to the modeling of the conditions in the shear-plane region. Thus, application of the analysis procedure to situations where a single large crack exists, or is likely to form, is not recommended unless the crack and reinforcement conditions are discretely modeled. In general, however, the modi-

fied compression field theory seems reasonably capable of predicting response in cases which deviate somewhat from the assumed conditions of smeared cracks and distributed reinforcement.

The shear-friction specifications of ACI 318 and CSA A23.3 were found to be generally conservative in predicting strengths for the test panels. However, in cases of compression and shear, where failure can be governed by a crushing of concrete, the code provisions of ACI 318 became less conservative and those of CSA A23.3 became unconservative.

The test panels demonstrated strengths substantially higher than did previously tested corresponding panels uniaxially reinforced throughout. This indicated that the nonlinear response of reinforced concrete can result in significant internal stress redistributions. The common design-checking procedure of examining local behavior on the basis of stresses determined from a linear elastic global analysis will not provide a proper account.

ACKNOWLEDGMENT

The work presented in this paper was made possible through funding from the Natural Sciences and Engineering Research Council of Canada. The authors wish to express their sincere gratitude for the support received.

NOTATION

E_s = modulus of elasticity of reinforcements
f'_c = compressive strength of concrete cylinder
f_{sp} = concrete cracking stress (split-cylinder)
f_x = normal stress applied on panel edges, x-direction
f_y = normal stress applied on panel edges, y-direction
f_{ys} = reinforcement yield stress
v = shear stress applied on panel edges
v_u = ultimate shear stress
ϵ_o = strain in concrete cylinder at press stress f'_c
ρ_x = steel reinforcement ratio in longitudinal direction
ρ_y = steel reinforcement ratio in transverse direction

REFERENCES

1. Vecchio, Frank J., and Collins, Michael P., "Modified Compression-Field Theory for Reinforced Concrete Elements Subjected to Shear," ACI JOURNAL, *Proceedings* V. 83, No. 2, Mar.-Apr. 1986, pp. 219-231.

2. Vecchio, Frank J., "Nonlinear Finite Element Analysis of Reinforced Concrete Membranes," *ACI Structural Journal,* V. 86, No. 1, Jan.-Feb. 1989, pp. 26-35.

3. Bhide, S. B., and Collins, M. P., "Reinforced Concrete Elements in Shear and Tension," *Publication* No. 87-20, Department of Civil Engineering, University of Toronto, 1987, 147 pp.

4. ACI Committee 318, "Building Code Requirements for Reinforced Concrete (ACI 318-83)," American Concrete Institute, Detriot, 1983, 111 pp.

5. "Design of Concrete Structures for Buildings (CSA A23.3-M84)," Canadian Standards Association, Rexdale, Ontario, 1984, 281 pp.

6. Hofbeck, J. A.; Ibrahim, I. O.; and Mattock, Alan H., "Shear Transfer in Reinforced Concrete," ACI JOURNAL, *Proceedings* V. 66, No. 2, Feb. 1969, pp. 119-128.

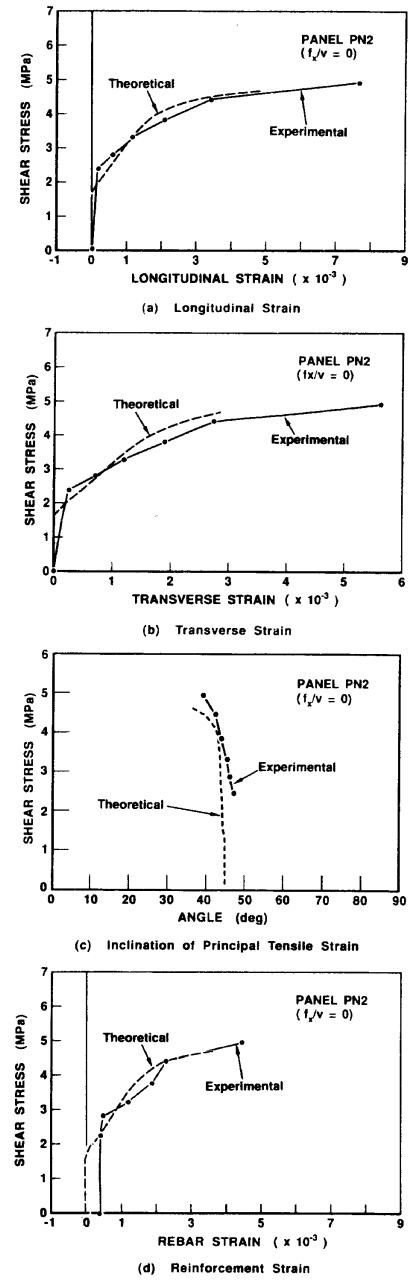

Fig. 10—Comparison of theoretical and experimental response for Panel PN2

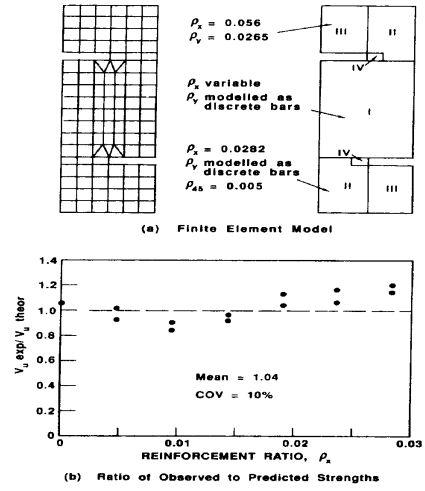

Fig. 11—Finite element analysis of pushoff specimens